Chemistry Europe
European Chemical Societies Publishing

High-Pressure Operando UV-Vis Micro-Spectroscopy of Coke Formation in Zeolite-based Catalyst Extrudates during the Transalkylation of Aromatics

Suzanna P. Verkleij,[a] Gareth T. Whiting,*[a] Sonia Parres Esclapez,[b] Shiwen Li,[b] Machteld M. Mertens,[b] Marcel Janssen,[b] Anton-Jan Bons,[b] Martijn Burgers,[b] and Bert M. Weckhuysen*[a]

The performance of zeolite-based catalyst extrudates can be largely influenced by the choice of binder material. To investigate these binder effects in zeolite-based catalyst extrudates in more detail, high spatiotemporal resolution techniques need to be further developed and employed. In this work, we present a new methodology to investigate binder effects in catalyst extrudates at different reaction pressures using *operando* UV-vis diffuse reflectance (DR) micro-spectroscopy coupled with on-line gas chromatography. We have studied mm-sized zeolite H-ZSM-5-containing extrudates with either Al_2O_3 or SiO_2 binder material, during the transalkylation of toluene with 1,2,4-trimethylbenzene at 450 °C and at a pressure of either 1 or 5 bar. Using this technique, it was revealed that the binder material significantly influenced catalyst deactivation at different reaction pressures. By subsequent mapping of the cross sections of the cylindrical catalyst extrudates using UV-vis micro-spectroscopy, it was shown that the SiO_2-bound extrudate formed poly-aromatic coke molecules homogeneously throughout the entire extrudate, whereas for the Al_2O_3-bound extrudate a coke ring formed that moved inwards with increasing reaction time. Notably, the developed methodology is not limited to the transalkylation reaction, and can also be used to gain more insight into binder effects during a variety of important catalytic reactions.

Introduction

Zeolite-containing catalyst extrudates are widely used in chemical processing, such as fluid catalytic cracking (FCC), alkane isomerization and aromatics alkylation reactions.[1–3] Catalyst extrudates are employed in large industrial reactors, as they can achieve high catalytic activity and selectivity, whilst maintaining high mechanical, chemical and thermal stability. To achieve these properties, zeolites are often mixed with different materials, such as a binder (e.g. amorphous alumina or silica) for mechanical strength.[4] Although these inorganic components are often not considered reactive, it has been reported that they can have a large influence (both beneficial or detrimental) on the activity, stability or selectivity of catalyst materials.[5–8]

Previous work has shown that a binder material can alter the acidity of a sample, which influences the performance of the catalyst.[9–11] Zhang *et al.*[12] investigated the influence of an alumina binder during dehydrogenation of propane on PtSnNa-ZSM-5 catalysts. They showed that the presence of the binder decreases the surface area of the catalyst, and, in addition, Al species from the binder were found to migrate into the zeolite framework to create extra acid sites. The alumina binder was found to influence both the activity and selectivity of the reaction. Whiting *et al.*[13] investigated the oligomerization of thiophene on either Al_2O_3- or SiO_2-bound zeolite H-ZSM-5-containing extrudates. They showed that the reaction mechanism was dependent on the choice of binder. With an Al_2O_3 binder, the ring opening mechanism (formation of thiol-like species) was favored, due to extra acid sites created under the influence of the binder. The formation of extra acid sites was confirmed by extruding a silicalite powder with Al_2O_3. Although both materials are inert during the thiophene reaction, the combination of materials forms thiol-like species due to the creation of extra acid sites. These examples illustrate the large impact of the binder material on the performance of catalyst extrudates, showing the importance of a thorough understanding of these complex interactions.

One of the challenges in studying zeolite-based extrudates is the large differences in dimensions, ranging from the (sub-)μm-sized zeolite material to the mm-sized catalyst extrudate itself. To overcome these differences in dimensions, advanced characterization techniques have been explored that can

[a] S. P. Verkleij, Dr. G. T. Whiting, Prof. B. M. Weckhuysen
Inorganic Chemistry and Catalysis
Debye Institute for Nanomaterials Science
Utrecht University
Universiteitsweg 99, 3584 CH Utrecht (The Netherlands)
E-mail: g.t.whiting@uu.nl
b.m.weckhuysen@uu.nl
[b] Dr. S. Parres Esclapez, Dr. S. Li, Dr. M. M. Mertens, Dr. M. Janssen, Dr. A.-J. Bons, Dr. M. Burgers
ExxonMobil Chemical Europe, Inc.,
European Technology Centre
Hermeslaan 2, B 1831 Machelen (Belgium)

Supporting information for this article is available on the WWW under https://doi.org/10.1002/cctc.202000948

investigate both μm-sized FCC particles and mm-sized catalyst extrudates non-invasively. Examples of these techniques are UV-vis diffuse reflectance micro-spectroscopy and confocal fluorescence microscopy, [13–16] focused-ion-beam scanning electron microscopy (FIB-SEM), [17] X-ray tomography (XRM), [18] X-ray diffraction computed tomography (XRD-CT)[19] and nano-secondary ion mass spectrometry (SIMS).[20] However, these characterization techniques have mainly been used to study model reactions or to elucidate catalytic reactions at relatively low or near ambient pressures.

The focus of this work is on the transalkylation of low-cost toluene with 1,2,4-trimethylbenzene (1,2,4-TMB), which is an interesting alternative to making the economically more attractive xylene.[21–25] Xylene (and mainly the isomers *p*-xylene and *o*-xylene) is used in the production of plastics, polyester fibers, resins and plasticizers. It is largely produced by steam cracking of heavy fractions and catalytic reforming of naphtha, but the transalkylation reaction is an attractive alternative method.[26,27] During the transalkylation process, toluene and 1,2,4-TMB can undergo several different reactions under the influence of a solid acid catalyst. These reactions include transalkylation, dealkylation, disproportionation and isomerization reactions, forming a mixture of products, including benzene, *m*-xylene, *p*-xylene, *o*-xylene, 1,2,3-TMB and 1,3,5-TMB.[28–30] Which of these different reaction pathways take place, is largely dependent on the acidity of the zeolite that is employed. Dumitriu *et al.*[31] showed that transalkylation and disproportionation mainly occur on strong acid sites, while isomerization can take place on weak acid sites. Isomerization reactions can decrease the *p*-xylene selectivity and transform the 1,2,4-TMB to less reactive and more bulky 1,3,5-TMB or 1,2,3-TMB.[32–36] Furthermore, the performance of the zeolite catalyst during the transalkylation reaction is also dependent on the reaction conditions that are used. Previous studies showed that the catalytic conversion increased with increasing pressure, as the higher pressure enhanced the adsorption of the reactants on the active sites of the catalyst. Furthermore, the xylene selectivity decreased with increasing pressure, as more side reactions can occur when the pressure is increased.[37,38] These side reactions cause the formation of poly-aromatic molecules, also known as coke molecules, that block the pores of the zeolite and cause deactivation.[27,39,40]

Previously, we have investigated mm-sized zeolite H-ZSM-5-containing extrudates, with either SiO_2 or Al_2O_3 as binder materials during the transalkylation reaction at atmospheric pressure. The different catalyst extrudates were compared using an *in-situ* UV-vis diffuse reflectance (DR) micro-spectroscopic and *ex-situ* confocal fluorescence microscopic approach.[41] Using these characterization techniques, coke species were revealed to predominantly form on the rim of zeolite H-ZSM-5 crystals within Al_2O_3-bound extrudates. By employing silicalite-containing Al_2O_3-bound extrudates, it was found that Al migration between the zeolite crystals and the Al_2O_3 binder creates additional acid sites near the zeolite external surface. Catalytic tests showed that these extra acid sites can isomerize the 1,2,4-TMB into more bulky 1,3,5-/1,2,3-TMB. Such sterically hindered species subsequently cause the formation of fluorescent coke species on the edge of the zeolite H-ZSM-5 crystals.

In this work we aim to take the next step and extend our work to higher reaction pressures, and develop a new analytical methodology to investigate binder effects with *operando* UV-vis DR micro-spectroscopy and on-line product analysis. More specifically, a microscopy reactor system, which can go to higher pressures (e.g. 5 bar), was developed, and installed under an UV-vis microscope in order to follow the deactivation of the catalyst extrudates and to investigate the influence of the binder material during the transalkylation of toluene and 1,2,4-TMB at two different pressures, namely 1 and 5 bar. The catalytic reaction was performed on the same zeolite H-ZSM-5-containing mm-sized extrudates bound with either SiO_2 or Al_2O_3, as investigated in our previous study.[41] The SiO_2-bound extrudate showed an increase in conversion at 5 bar, which caused the formation of more poly-aromatic molecules that are homogeneously distributed throughout the extrudate. However, for the Al_2O_3-bound catalyst extrudate, the poly-aromatic molecules formed in a ring inside the extrudate, which became more extensive under influence of a higher pressure. This new method of investigating binder effects in extrudates can be used to study binder effects during different reactions on a large range of catalyst extrudates.

Results and Discussion

Characterization of the catalyst materials under study

The catalyst extrudates under study were analyzed with Ar physisorption, scanning electron microscopy with energy dispersive X-ray spectroscopy (SEM-EDX) and NH_3 temperature programmed desorption (TPD). Table 1 shows the BET surface

Table 1. Brunauer-Emmett-Teller[a] (BET) surface areas and [b]pore volumes of the different catalyst samples under investigation, measured with Ar physisorption. [c]Quantity of NH_3 per g, measured with NH_3 temperature programmed desorption (NH_3 TPD). The predicted surface area, pore volumes and acidity are calculated with the ratio of the pure components and are shown between parentheses. [d]wt.% of coke after 1 h of transalkylation reaction at 450 °C on the catalyst extrudate, measured with thermogravimetrical analysis (TGA).

	H-ZSM-5 : binder [wt.%]	Binder	BET surface area [m^2/g][a]	Pore volume [cm^3/g][b]	Micropore volume [cm^3/g][b]	NH_3 TPD [mmol/g][c]	[wt.%] coke at 1 bar[d]
H-ZSM-5	100:0	–	374	0.19	0.13	0.48	5
SiO_2	0:100	SiO_2	184	0.32	0	0.02	1
Al_2O_3	0:100	Al_2O_3	209	0.47	0	0.45	7
20:80 SiO_2	20:80	SiO_2	221 (222)	0.28 (0.29)	0.03	0.12 (0.11)	2
20:80 Al_2O_3	20:80	Al_2O_3	241 (242)	0.49 (0.41)	0.03	0.46 (0.46)	7

area and (micro)pore volume of the studied samples measured with Ar physisorption. The BET surface area and micropore volume decreases when a binder is added to the zeolite H-ZSM-5, due to the dilution of the samples (i.e. the BET surface area of the H-ZSM-5 powder, 374 m^2/g, is higher than that of 20:80 SiO_2, 221 m^2/g, and 20:80 Al_2O_3, 241 m^2/g). However, the total pore volume increases with higher binder content, due to the larger pores present in the binder. The predicted surface area is in good agreement with the experimental data, showing no severe pore blocking due to the addition of the binder. The zeolite H-ZSM-5 distribution throughout the 20:80 Al_2O_3 extrudate was measured with SEM-EDX and are shown in Figure S1. The analysis shows that the zeolites are homogeneously distributed throughout the 20:80 Al_2O_3 extrudate. NH_3 TPD was used to study the acidity of the different samples and the results are shown in Table 1. The 20:80 SiO_2 extrudate has a lower concentration of acid sites than the 20:80 Al_2O_3 extrudate as the Al_2O_3 binder itself contains acid sites, but the acid concentration are similar to the predicted values (the predicted values are composed of 20% of the H-ZSM-5 and 80% of the binder).

Transalkylation reaction at 1 bar and 5 bar of reaction pressure

Using our newly developed analytical methodology, the catalyst activity and deactivation was followed with *operando* UV-vis diffuse reflectance (DR) micro-spectroscopy and on-line product analysis at different reaction pressures, namely 1 and 5 bar. First, we will discuss the UV-vis DR micro-spectroscopy results and subsequently link these spectroscopic data to the product formation, as measured with on-line gas chromatography.

Using *operando* UV-vis DR micro-spectroscopy, the hydrocarbon species formed on the surface of the catalyst extrudates were analyzed. Figure 1 shows the *operando* UV-vis DR spectra during 1 h of the transalkylation reaction. UV-vis DR spectroscopy can be used to determine different types of hydrocarbon species on the surface of the catalyst extrudate, as different kinds of organic molecules absorb light at different wavenumbers (Figure 1a). The neutral reactants and reaction products, like toluene, 1,2,4-trimethylbenzene (1,2,4-TMB) and xylene have an absorption band at around 40000 cm^{-1} (250 nm), and only the tail of this absorption band can be distinguished in the UV-vis DR spectra. During the reaction, the reactants form charged alkylated aromatics, which are reaction intermediates, that have an absorption band around 28000 cm^{-1} (350 nm).[24,43,44] The more conjugated the organic molecules become, the lower the absorption wavenumber. Large polyaromatic molecules have an absorption band at around

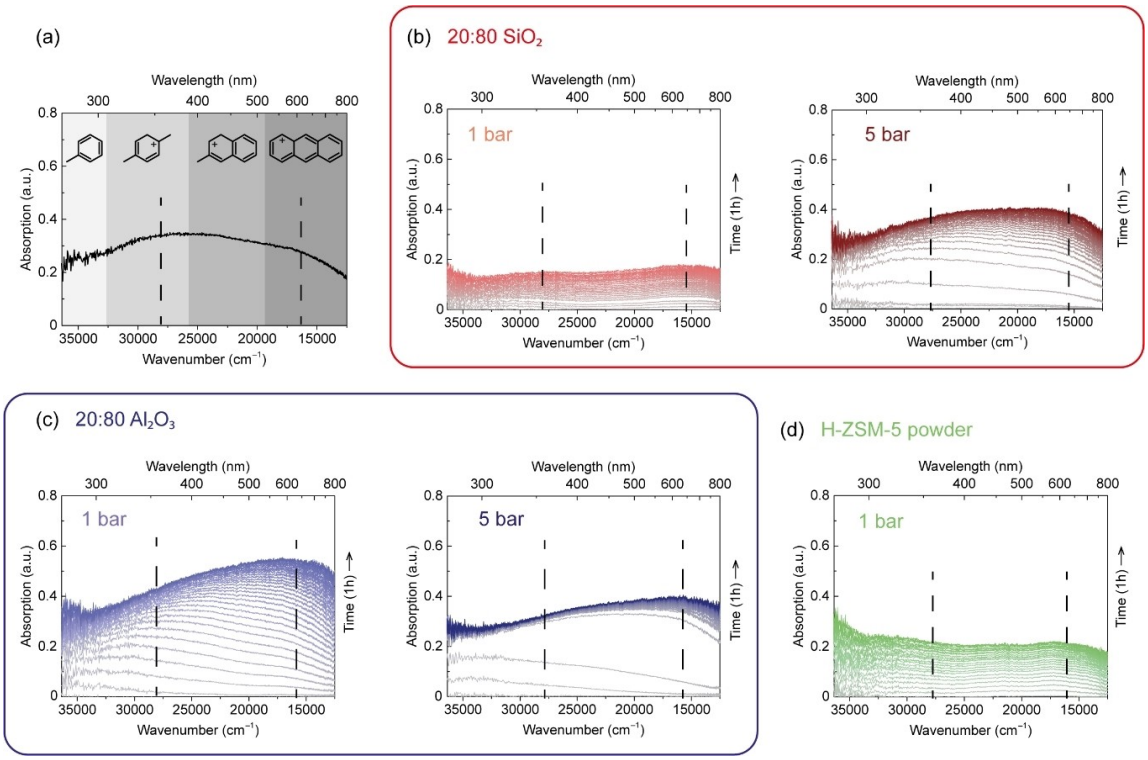

Figure 1. (a) Schematic of different regions that increase in absorption in the UV-vis diffuse reflectance (DR) spectra during the reaction of toluene and 1,2,4-trimethylbenzene (1,2,4-TMB). In the different spectral regions, an example of the type of molecule that absorbs the light is presented. *Operando* UV-vis DR spectroscopy during the transalkylation of toluene with 1,2,4-TMB at 450 °C on (b) 20:80 Al_2O_3 extrudates at 1 bar and 5 bar (c) 20:80 SiO_2 extrudates at 1 bar and 5 bar, and (d) H-ZSM-5 at 1 bar. The UV-vis DR spectra were taken every 2 min for 1 h of reaction time.

16500 cm^{-1} (600 nm), and these poly-aromatic molecules, also known as coke molecules, block the pores of the zeolite and hence deactivate the catalyst.[27,39,40] However, the UV-vis DR absorption bands are broad as a lot of different hydrocarbons are formed on the surface of the extrudate which have overlapping absorption bands and therefore only absorption regions are discussed.

Figure 1b and c show the *operando* UV-vis DR spectra of the H-ZSM-5-containing extrudates bound with SiO_2 and Al_2O_3. During the transalkylation reaction on 20:80 SiO_2 at 1 bar (Figure 1b), an absorption band appears in the region around 28000 cm^{-1} (350 nm) due to the formation of charged alkylated aromatics (reaction intermediates) or small coke molecules. The absorption band shifts to lower wavenumbers as the organic molecules become more conjugated and form coke molecules. Subsequently, an absorption band appears in the region around 16500 cm^{-1} (600 nm) due to the formation of poly-aromatic molecules, which block the pores of the zeolite and deactivate the catalyst material. By comparing the *operando* UV-vis DR spectra of the 20:80 SiO_2 to the UV-vis DR spectra of 20:80 Al_2O_3 (Figure 1c), it becomes apparent that the absorption is much higher in intensity for the Al_2O_3-bound catalyst extrudate, both for the charged alkylated aromatics or small coke molecules with an absorption region around 28000 cm^{-1} (350 nm) and the large poly-aromatic molecules with an absorption region around 16500 cm^{-1} (600 nm). This difference can be largely explained by the difference in binder material. SiO_2 on itself does not have any acid sites, and the UV-vis DR spectra (Figure S2a) consequently do not form any absorption bands during the reaction. The UV-vis DR spectra of 20:80 SiO_2 (Figure 1b) resemble therefore the UV-vis DR spectra of the zeolite H-ZSM-5 powder (Figure 1d), showing that the SiO_2 binder has not much influence on the type of hydrocarbon molecules formed on the surface of the catalyst extrudate. On the other hand, the Al_2O_3 binder itself does contain weak acid sites, which can form charged alkylated aromatics. The UV-vis DR spectra of the pure 100 Al_2O_3 binder extrudate in Figure S2b thus display a large absorption band at around 28000 cm^{-1} (350 nm), which becomes more intense and shifts to lower wavenumbers, showing the presence of charged alkylated aromatics.

To confirm if the Al_2O_3-bound catalyst extrudates contain more conjugated coke molecules after reaction, the amount of residue on the reacted samples was analyzed with thermogravimetric analysis (TGA) (Table 1). At 1 bar, the 20:80 Al_2O_3 contains 7 wt.% of residue, which is more than the 20:80 SiO_2 sample that contains 2 wt.% of residue. This confirms the UV-vis DR results that show more large conjugated species formed on the surface of the 20:80 Al_2O_3 catalyst extrudate.

Figure 2a compares the UV-vis DR spectrum of the 20:80 Al_2O_3 binder after 1 h of reaction to the predicted spectrum. The predicted spectrum is composed of 20% of the UV-vis DR spectrum of the zeolite H-ZSM-5 and 80% of the UV-vis DR spectrum of the Al_2O_3 binder. The UV-vis DR spectrum of the 20:80 Al_2O_3 extrudate has a higher absorption around 600 nm, and this extra absorption indicates a more extensive formation of poly-aromatic molecules. Previous characterization studies have shown that extra acid sites can be formed at the zeolite-binder interface under the influence of an Al_2O_3 binder.[10–13] These additional acid sites could explain the enhanced formation of poly-aromatic molecules. Furthermore, the 20:80 SiO_2 UV-vis DR spectrum, in Figure 2b, shows an increase in absorption compared to the predicted spectrum, but does not have a large difference in absorption bands which indicates that the SiO_2 binder does not change the selectivity of the catalyst extrudate. The increase in absorption can be caused by an increase in conversion due to the larger pore size of the catalyst extrudate.

Figure 1 also compares the UV-vis DR spectra of the 20:80 Al_2O_3 and 20:80 SiO_2 for the reactions at 1 bar and 5 bar of pressure. By comparing these UV-vis DR spectra it becomes clear that the absorption bands are formed at a greater rate at 5 bar, indicating a higher conversion level at 5 bar. The higher pressure forces more reactants onto the catalytic active sites,

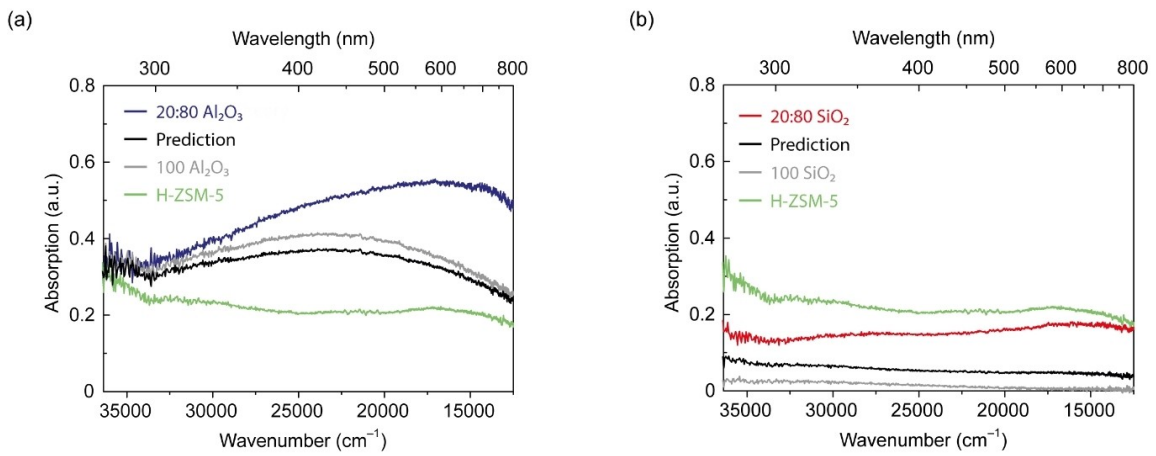

Figure 2. UV-vis diffuse reflectance (DR) spectra after 1 h of transalkylation reaction with toluene and 1,2,4-trimethylbenzene (1,2,4-TMB) at 450 °C and at 1 bar of pressure of H-ZSM-5-containing binder-bound extrudate (blue or red), pure binder extrudate (grey) and H-ZSM-5 powder (green). The predicted UV-vis spectra (black) are a combination of 20% of the H-ZSM-5 UV-vis DR spectrum and 80% of the pure binder UV-vis DR spectrum. These UV-vis DR spectra are shown for (a) the Al_2O_3 binder and (b) the SiO_2 binder.

therefore increasing the activity of the catalyst.[37,38] Furthermore, the intensity of the absorption bands is higher for the 20:80 SiO_2 5 bar reaction than for the 1 bar reaction as more polyaromatic species are formed due to a higher conversion. However, the intensity of the absorption bands does not increase for the 20:80 Al_2O_3 catalyst extrudate between 1 bar and 5 bar of reaction pressure. This could indicate that for both pressures all the active sites on the surface of the extrudate contain coke molecules and no more coke molecules can be formed on the surface of the extrudate.

To correlate the UV-vis DR spectral analysis with the formation of the reaction products leaving the extrudates, an on-line gas chromatograph was directly coupled to the reaction cell (Experimental Section, Figure 8). Figure 3 shows the time-resolved conversion during the transalkylation reaction compared to the time-resolved intensity of the UV-vis DR absorption bands. As soon as the transalkylation reaction starts, an absorption region at 28000 cm^{-1} (350 nm) is formed, which corresponds to an increase in conversion. The difference in conversion between the 20:80 SiO_2 extrudates reacted at 1 bar of pressure (Figure 3a) to the extrudates reacted at 5 bar of pressure (Figure 3b) confirms that a larger increase in the 28000 cm^{-1} (350 nm) absorption intensity corresponds to a higher conversion. After the initial increase of conversion, an absorption region around 16500 cm^{-1} (600 nm) is formed due to the creation of large poly-aromatic molecules. For the 20:80 SiO_2 extrudates, the formation of poly-aromatic molecules corresponds to a decrease in conversion, which shows that these molecules cause the deactivation of the catalyst extrudate.

However, for the 20:80 Al_2O_3 reacted at 1 bar of pressure (Figure 3c), the formation of poly-aromatic molecules does not correspond to a decrease in conversion. After the initial increase, both the conversion and absorption band intensity are constant and no deactivation is visible. This increase in the 16500 cm^{-1} absorption band is faster at 5 bar, and after 7 min the intensity of this absorption band hardly increases indicating that the maximum concentration of poly-aromatic molecules is formed at the surface of the catalyst extrudate. However, this does not correspond with the deactivation of the extrudate, as the conversion only slightly decreases. This difference between the 20:80 Al_2O_3 extrudate and the 20:80 SiO_2 extrudate indicates a difference in extrudate deactivation due to a binder effect.

Figure 3 shows that the conversion is not only higher for the reactions at 5 bar, but the conversion is also higher for the 20:80 Al_2O_3 extrudates compared to the 20:80 SiO_2 extrudates. To investigate if the selectivity is also different, the xylene yield per g of catalyst and the 1,3,5-TMB yield per g of catalyst is shown in Figure 4. Although the conversion is higher for 20:80 Al_2O_3 extrudates, the xylene yield is similar for all catalyst extrudates. The higher conversion of the 20:80 Al_2O_3 extrudate

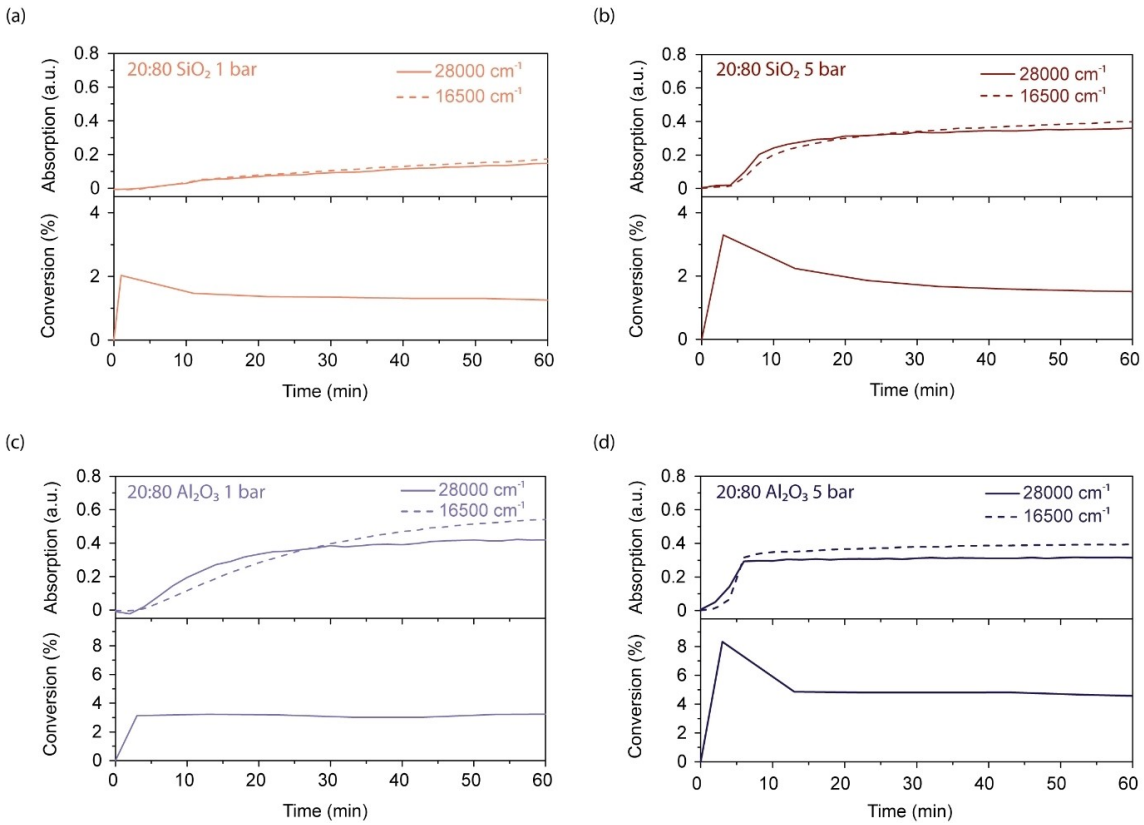

Figure 3. Comparison of the UV-vis intensity profiles of 28000 cm^{-1} (350 nm) (solid line), and 16500 cm^{-1} (600 nm) (dotted line) absorptions and the conversion for the (a) 20:80 Al_2O_3 extrudate at 1 bar, (b) 20:80 Al_2O_3 extrudate at 5 bar, (c) 20:80 Al_2O_3 extrudate at 1 bar and (d) 20:80 Al_2O_3 extrudate at 5 bar during the transalkylation of toluene with 1,2,4-trimethylbenzene for 1 h at 450 °C and 2 h^{-1} WHSV.

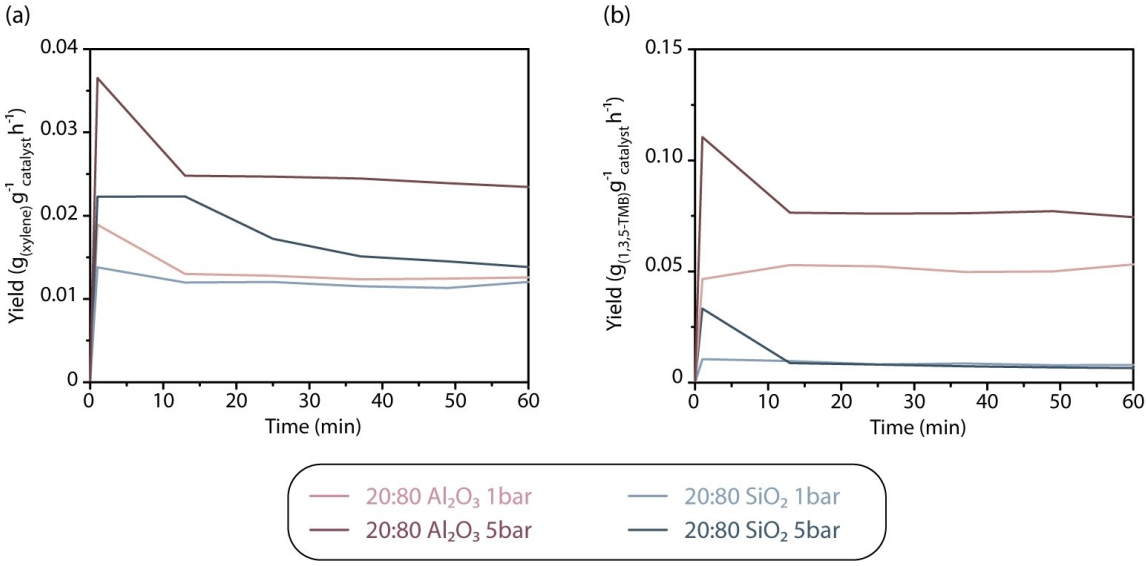

Figure 4. (a) Xylene yield and (b) 1,3,5-trimethylbenzene (TMB) yield as a function of time on stream, during the transalkylation reaction of toluene and 1,2,4-TMB over the 20:80 SiO_2 extrudate at 1 bar (light red), 20:80 SiO_2 extrudate at 5 bar (dark red), 20:80 Al_2O_3 extrudate at 1 bar (light blue), 20:80 Al_2O_3 extrudate at 5 bar (dark blue) at 450 °C and 2 h^{-1} WHSV.

is due to an increase in 1,2,4-TMB isomerization. To investigate if the difference in activity and selectivity is due to binder itself or due to the combination of the components, the individual materials of the catalyst extrudates were also investigated and compared to the 20:80 Al_2O_3 and 20:80 SiO_2 extrudates (Figure S3). The H-ZSM-5 powder has a conversion of 4% and has a xylene yield of 0.02 $g_{xylene}/g_{catalyst}$ and is therefore the active component in the catalyst extrudate. Both the SiO_2 and Al_2O_3 binder have almost no activity during the transalkylation, and the increase in isomerization products for the 20:80 Al_2O_3 extrudate must therefore be due to an effect which occurs upon the combination of the H-ZSM-5 zeolite and the Al_2O_3 binder. Previously it was reported that under influence of an Al_2O_3 binder, Al species can migrate between het H-ZSM-5 crystals and the binder, forming extra acid sites.[13] The increase in isomerization products can be attributed to the extra acid sites formed between the H-ZSM-5 crystals and the binder.[41]

Characterization of the coke deposition throughout the catalyst extrudate

To investigate if the extensive formation of poly-aromatic molecules was homogeneous throughout the catalyst extrudates, cross sections of the different extrudates were measured. Figure 5 shows the photographs and UV-vis diffuse reflectance (DR) micro-spectroscopy mapping of the cross sections of the 20:80 SiO_2 and 20:80 Al_2O_3 extrudates reacted for 1 h at 1 bar and 5 bar. The photographs of the catalyst extrudate cross sections show that the 20:80 SiO_2 extrudate has a homogeneous color throughout the extrudate for both the reaction at 1 bar (Figure 5a) and 5 bar (Figure 5b). This indicates that the deactivating poly-aromatic molecules are homogeneously formed throughout the catalyst extrudate. In the middle of the image, the absorption at 28000 cm^{-1} (350 nm) (compared to the center of the extrudate) is mapped through the extrudate. The absorption band at 28000 cm^{-1} (350 nm) is formed due to the presence of charged alkylated aromatics, a reaction intermediate for the transalkylation reaction and/or small coke molecules. The UV-vis DR map in the center therefore shows that the charged alkylated aromatics are distributed homogeneous through the catalyst extrudate, for both the 1 bar (Figure 5a) and 5 bar (Figure 5b) reaction. In the right image, the ratio of the absorption at 16000 cm^{-1} (600 nm) to 28000 cm^{-1} (350 nm) is mapped across the catalyst extrudates. Poly-aromatic molecules absorb light at 600 nm, whereas the charged alkylated aromatics and small coke molecules absorb light at 350 nm. An increase in the 600 nm to 350 nm absorption ratio is indicative for a higher amount of poly-aromatic molecules, compared to the smaller hydrocarbon species. The 20:80 SiO_2 extrudate has a similar ratio throughout the catalyst extrudate, showing that the concentration of large poly-aromatic molecules is equal throughout the catalyst extrudate. This explains the gradual decrease in conversion, with the gradual formation of poly-aromatic molecules through the catalyst extrudate.

In contrast to the 20:80 SiO_2 extrudate, the photograph of the 20:80 Al_2O_3 extrudate cross section shows a dark color on the edge of the extrudate for both the reaction at 1 bar (Figure 5c) and 5 bar (Figure 5d), and this difference is confirmed with UV-vis DR micro-spectroscopy. The absorption at 28000 cm^{-1} (350 nm), due to charged alkylated aromatics or small coke molecules, is higher at the edge compared to the centre of the extrudate. Furthermore, the ratio of the absorption at 16000 cm^{-1} (600 nm) to 28000 cm^{-1} (350 nm) is higher at the edge of the extrudate compared to the center, indicating an

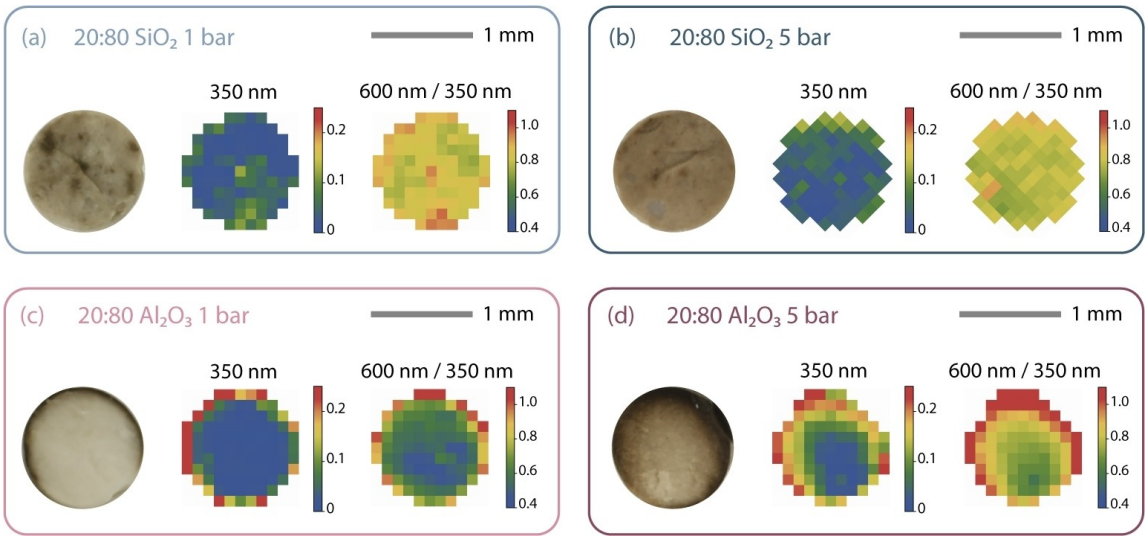

Figure 5. Cross sections of different catalyst extrudates after transalkylation reaction with toluene and 1,2,4-trimethylbenzene during 1 h on (a) the 20:80 SiO_2 extrudates at 1 bar, (b) the 20:80 SiO_2 extrudates at 5 bar, (c) the 20:80 Al_2O_3 extrudates at 1 bar and (d) the 20:80 Al_2O_3 extrudate at 5 bar. The figures show on the left a photograph of the catalyst extrudates, in the center a UV-vis map of the absorption intensity at 350 nm compared to the center of the catalyst extrudate and on the right a map of the intensity ratio of the 600 and 350 nm UV-vis absorption bands. The size of the pixels in the UV-vis maps is 110×110 μm and the reactant flow is from the top to the bottom of the catalyst extrudate.

increase in large poly-aromatic molecules on the edge of the catalyst extrudate. Comparing these results for the 1 bar reaction (Figure 5c) to the 5 bar reaction (Figure 5d) shows that the dark edge of the 20:80 Al_2O_3 reacted at 1 bar is smaller (around 100 μm) than the edge of the extrudate reacted at 5 bar (around 350 μm). However, from only these microscopy results it is not clear if the ring formation is due to the accessibility of the catalyst extrudate itself or due to the higher conversion, limiting the diffusion of the coke molecules.

Recently, Whiting *et al.*[45] showed that for the methanol-to-hydrocarbon (MTH) reaction a ring of large poly-aromatic molecules is formed due to a boundary inside the catalyst extrudate. They investigated this boundary by measuring the diffusion of a series of fluorescent dye molecules, differing in their molecular size, through catalyst extrudates containing different clay minerals as binders. To investigate if the ring formation in the 20:80 Al_2O_3 extrudate under study is due to accessibility differences between the Al_2O_3 and SiO_2 based extrudates, the mobility of a fluorescent dye was measured through the extrudates. The fluorescent dye molecule, *N*,*N*′-Bis (1-hexylheptyl)-perylene-3,4:9,10-bis-(dicarboximide) having a size of ~2 nm, was diluted in toluene and added to the catalyst extrudates for different time intervals. Subsequently, the catalyst extrudate was dried and cut open and the penetration depth of the dye was measured with confocal fluorescence microscopy using a 488 nm laser to excite the samples. Figure 6

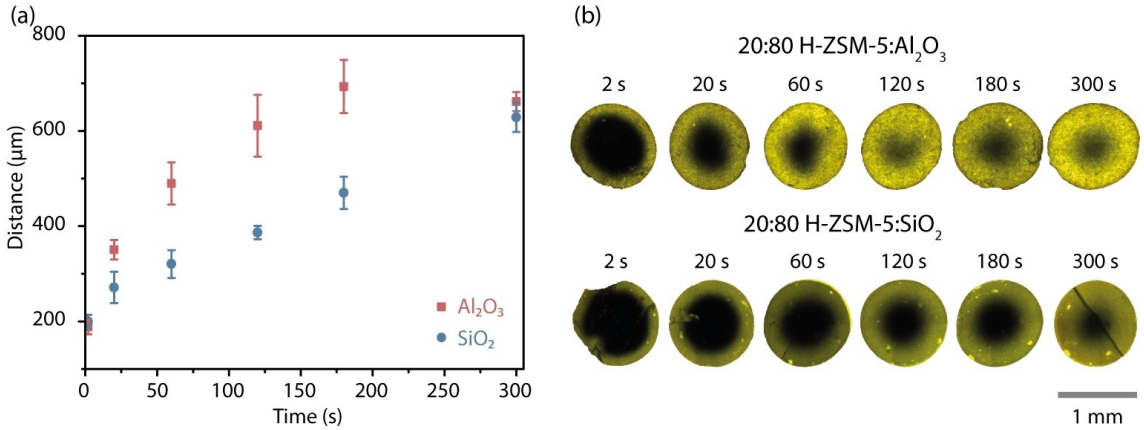

Figure 6. (a) Uptake (accessibility) studies of ~2 nm fluorescent nanoprobes versus time in the 20:80 Al_2O_3 extrudate (red) and the 20:80 SiO_2 extrudate (blue). The error bars are based on 8 probe penetration depth measurements for two separate catalyst extrudates. (b) 3-D confocal fluorescence microscopy images from different incubation time intervals for both the 20:80 Al_2O_3 and 20:80 SiO_2 extrudate, providing a visual representation of the fluorescent probe uptake.

shows that the accessibility for the 20:80 Al_2O_3 extrudate is significantly higher than for the 20:80 SiO_2 extrudate. For the 20:80 Al_2O_3 extrudate, the fluorescent dye almost completely penetrates the catalyst extrudate after 120 s, whereas for the 20:80 SiO_2 extrudate it takes 300 s. This shows that the difference in coke formation between the 20:80 Al_2O_3 extrudate and the 20:80 SiO_2 extrudate is not due to the accessibility of the catalyst extrudate.

The deactivation profile of the 20:80 Al_2O_3 extrudate can be attributed to the higher conversion and increased side reactions because of the acid sites in the binder and the extra acid sites formed between the binder and the zeolite. The increase in side reactions accelerates the coke formation and does not allow the reactants to diffuse completely through the catalyst. This would mean that the ring of coke molecules gradually moves inside the extrudates. To investigate if this is indeed the case, the Al_2O_3-bound catalyst extrudate was reacted with toluene and 1,2,4-TMB for 10 min, 30 min, 1 h and 3 h. Figure 7 shows the photographs and UV-vis absorption maps at 28000 cm^{-1} (350 nm) and 16500 cm^{-1} (600 nm) of the different reaction times for the 20:80 Al_2O_3 extrudate. The photographs show an increasingly darker ring formed on the 20:80 Al_2O_3 extrudate. Moreover, the UV-vis absorption maps show an increase in intensity and thickness of both the 28000 cm^{-1} (350 nm) and 16500 cm^{-1} (600 nm) absorption band, due to small and large coke molecules, respectively. Figure 7b shows that the ring at 28000 cm^{-1} due to small coke molecules is 33 μm after 10 min of reaction which increases to 62 μm after 30 min of reaction, 95 μm after 1 h and 120 μm after 3 h of transalkylation reaction. These results confirm that the ring is formed because the transalkylation reaction occurs fast compared to the diffusion through the extrudate, where the fast reaction rate is due to a binder effect of the Al_2O_3 binder. As a result, the ring of coke molecules gradually moves inside the extrudate, which means that the maximum concentration of poly-aromatic molecules is reached first at the surface of the extrudate, where the UV-vis DR spectra are measured. However, the center of the catalyst is still active, which explains the lack of deactivation shown in the conversion (Figure 3).

The combination of experimental approaches presented in this work can give more insight into binder effects at different pressures. For the transalkylation reaction, it showed that both the conversion and deactivation of the catalyst extrudate at different pressures is significantly influenced by the choice of binder. This method is not limited to the transalkylation reaction and can give insights into other chemical reactions and catalyst compositions. Considering the large influence of the type of binder on the conversion and deactivation for this study and potentially the selectivity for different chemical reactions, it becomes clear that it is vital to gain more insights into the effect of the binder on the reaction.

Conclusion

A new high-pressure *operando* UV-Vis diffuse reflectance (DR) micro-spectroscopy method with on-line product analysis has been developed to investigate binder effects in catalyst extrudates at elevated pressures. Using this method, binder effects were investigated during the transalkylation of toluene and 1,2,4-trimethylbenzene (1,2,4-TMB) at 450 °C and at pressures of 1 and 5 bar on mm-sized H-ZSM-5-containing extrudates with two different binders, namely Al_2O_3 and SiO_2. The *operando* UV-vis DR absorption spectra showed that the 20:80 Al_2O_3 extrudate formed more extended poly-aromatic species than the catalyst extrudate with the SiO_2 binder. This

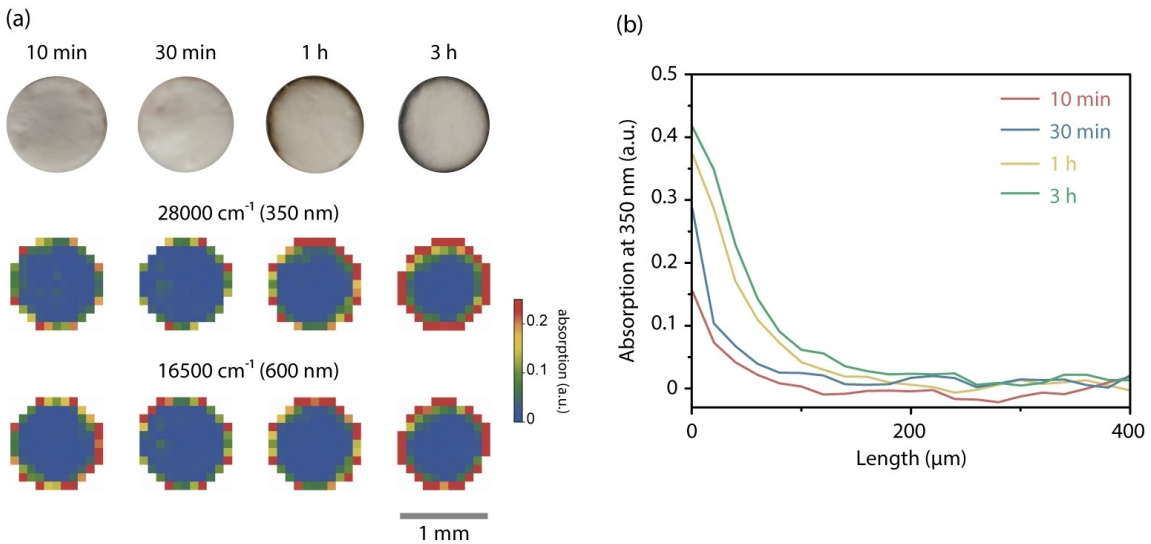

Figure 7. (a) Cross sections 20:80 Al_2O_3 extrudates after transalkylation reaction with toluene and 1,2,4-trimethylbenzene (1,2,4-TMB) for 10 min, 30 min, 1 h and 3 h. The figure shows on the top a photograph of the catalyst extrudates, in the center the UV-vis absorption map with the absorption intensity at 28000 cm^{-1} (350 nm) and on the bottom at 16500 cm^{-1} (600 nm). The size of the pixels in the UV-vis absorption maps is 110×110 μm, and the reactant flow is from the top to the bottom of the extrudate. (b) The absorption at 350 nm plotted for the first 400 μm of the 20:80 Al_2O_3 extrudate after transalkylation reaction for 10 min (red), 30 min (blue), 1 h (yellow) and 3 h (green).

difference cannot be explained by the presence of the acid sites in the Al_2O_3 binder, and was due to the creation of extra acid sites when zeolite H-ZSM-5 is combined with an Al_2O_3 binder. These extra acid sites also caused an increase in the amount of isomerization products for the 20:80 Al_2O_3 extrudate. When the reaction pressure was increased from 1 to 5 bar, the conversion was increased, which explained the faster formation of the UV-vis absorption bands. Although the formation of absorption bands was faster at 5 bar, the intensity of the absorption bands was only higher for the 20:80 SiO_2. The 20:80 Al_2O_3 extrudate had similar absorption band intensities after 1 h of reaction at 1 and 5 bar. Although the maximum concentration of coke molecule formation was reached at the surface, no deactivation of the 20:80 Al_2O_3 extrudate was observed as the coke migrated from the outside inwards. This is in contrast with the 20:80 SiO_2 extrudate, where the residue was homogeneously distributed throughout the extrudate. The difference in deactivation was not due to the accessibility of the catalyst extrudate, but caused by an increase in side reactions due to the extra acid sites, which does not allow the reactants to diffuse completely through the catalyst. Using this new method, we were able to measure the effect of the binder during the transalkylation reaction at different pressures. As binder effects play an important role in heterogeneous catalysis, the developed method can be used to detect binder effects in a wide variety of catalyst extrudates for different chemical reactions.

Experimental Section

The transalkylation reaction with toluene and 1,2,4-trimethylbenzene (1,2,4-TMB) was investigated at 450 °C for different pressures. A schematic of the developed and used reaction setup is shown in Figure 8. The reactions were performed in a CCR1000 Linkam Scientific Instruments cell coupled with a TMS94 temperature controller and a PSU1500 unit from Linkam Scientific Instruments. The reactor was fitted with a back-pressure regulator to perform reactions at 5 bar. Prior to reaction, around 20 mg of extrudates were calcined at 500 °C with O_2/N_2 for 1 h, and subsequently, the temperature was reduced to 450 °C for reaction. Toluene and 1,2,4-TMB were put in separate bubblers, and N_2 was flown through to evaporate the reactants in a 1:1 molar ratio with a WHSV of 2 h^{-1}. During transalkylation, the reaction products were measured with on-line gas chromatography (GC), and the hydrocarbon species formed on the surface of the extrudates were followed with UV-vis diffuse reflectance (DR) micro-spectroscopy. The reaction products were measured on an Interscience CompactGC$^{4.0}$ equipped with an MXT-5 column, 1 u 15 m * 0.28 mm and the response factor for the GC components was assumed to be 1. The microscopy reactor was mounted under a CRAIC 20/30 PV^{TM} micro-spectrophotometer equipped with a 15×0.28 NA reflective lens and a 30 W halogen lamp. The *operando* UV-vis DR spectra were measured on a 82×82 μm region on the external surface of the catalyst extrudate and spectra were recorded every 2 min for 1 h.

After catalytic reaction, the residue formed inside the catalyst extrudates was characterized with a combination of UV-vis DR micro-spectroscopy and thermogravimetrical analysis (TGA). UV-vis DR microscopy mapping was done on the same CRAIC 20/30 PV^{TM} micro-spectrophotometer, and the related spectra were taken on a

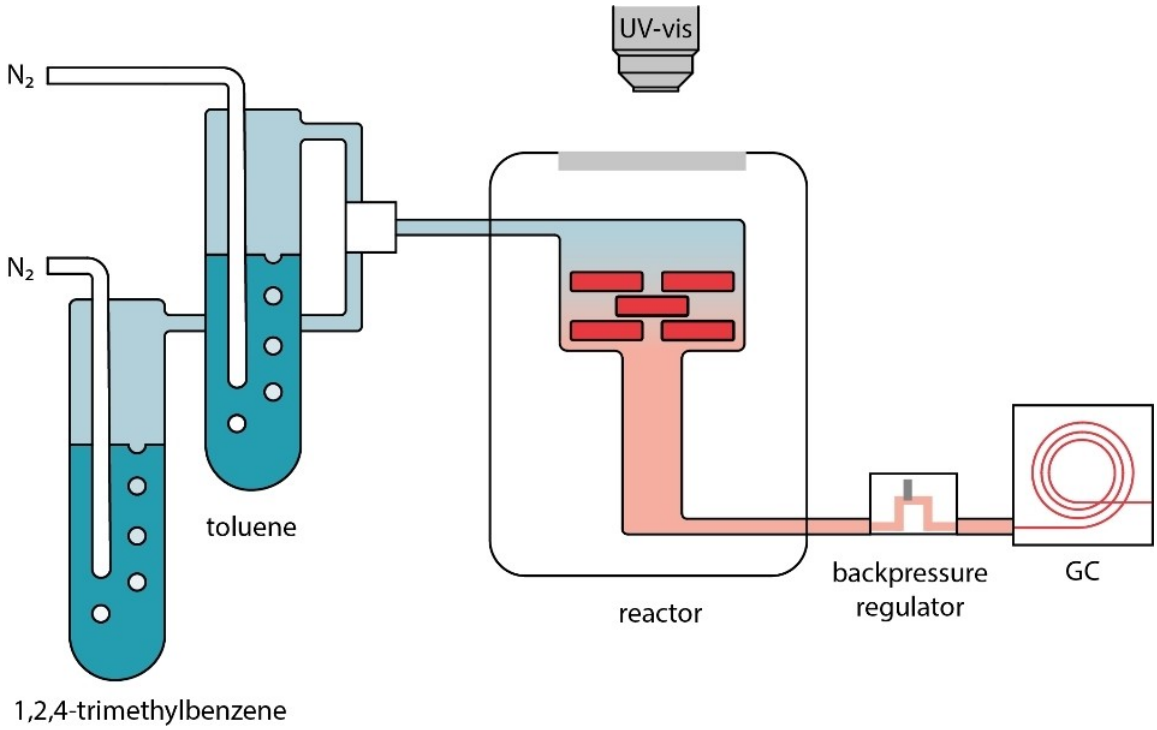

Figure 8. Schematic representation of the experimental setup. N_2 is bubbled separately through toluene and 1,2,4-trimethylbenzene (1,2,4-TMB) and mixed before it is flown into the reactor. The toluene and 1,2,4-TMB react with the catalyst extrudate at 450 °C, and the formed molecules on the catalyst extrudates are characterized with *operando* UV-vis diffuse reflectance (DR) micro-spectroscopy at elevated reaction pressures. After the reactants and products have gone through a backpressure regulator, they are measured with on-line gas chromatography (GC).

110×110 μm region. The hydrocarbon deposits inside the catalyst extrudate were characterized with TGA. The samples were heated to 700 °C with 5 °C/min under 10 ml/min O_2 on a PerkinElmer pyris 1 TGA instrument.

The transalkylation reaction was performed on zeolite H-ZSM-5-containing, SiO_2- or Al_2O_3-bound catalyst extrudates that were prepared by ExxonMobil according to example 1 in patent US6,039,864.[42] SiO_2 and Al_2O_3 were chosen as a binder material as they are widely used in industrial catalysts. The zeolite ZSM-5 crystals with an average crystal size of 3 μm and a Si/Al ratio of 32 were used together with SiO_2 gel (AEROSIL 300) and silica sol (NALCOAG 1034A) to form SiO_2-bound extrudates, and pseudo-boehmite alumina (Versal 300) was used to form Al_2O_3-bound extrudates. The zeolite ZSM-5 crystals and binder material were mixed with H_2O and an extrusion aid. This mixture was extruded into 1 mm-sized catalyst extrudates, dried overnight at 130 °C, and calcined at 500 °C for 18 h. Ion-exchange was performed by suspending the catalyst extrudates in a 1 M ammonium nitrate solution for 4 h, followed by washing and drying and a final calcination at 500 °C for 18 h. The different catalyst samples were named as follows: 'a:b binder c bar', for example '20:80 SiO_2 5 bar' is the 20 wt.% H-ZSM-5-containing 80 wt.% SiO_2-bound extrudate that was reacted at 5 bar during the transalkylation reaction. Not only the zeolite H-ZSM-5-containing extrudates were used in the transalkylation reaction, but also catalyst extrudates containing only binder and H-ZSM-5 powder.

The different catalyst materials under study were further characterized with Ar physisorption, NH_3 temperature programmed desorption (NH_3 TPD), scanning electron microscopy with energy dispersive x-ray spectroscopy (SEM-EDX) and the diffusion of probe molecules. Ar physisorption was used to determine the surface area and pore volume and was measured with a Micromeritics TriStar 3000 at 77 K. Prior to the measurement, the samples were dried under vacuum at 300 °C overnight. The surface area was calculated with the Brunauer-Emmett-Teller (BET) method, and the *t*-plot method was used to determine the pore volume. Before acidity measurements with NH_3 TPD, the samples were first dried at 550 °C under He flow, with a heating rate of 10 °C/min for 15 min. The NH_3 TPD was measured on a Mettler Toledo TGA/SDTA 851, and the samples were exposed to 12 pulses of 10% NH_3 in He at 100 °C. The desorption data was obtained by applying a temperature ramp of 5 °C/min to 550 °C under He flow. The amount of desorbed ammonia was monitored with a thermal conductivity detector (TCD). SEM-EDX was used to characterize the zeolite crystals inside the extrudate. An extrudate cross section was attached to a SEM stub and coated with Pd/Pt in a cressington 208HR sputter coater, and the extrudate was imaged on FEI Helios Nanolab G3 instrument.

The diffusivity of the samples was measured by putting the catalyst extrudates in a solution with a fluorescent dye for 6 different time periods (5 s, 20 s, 60 s, 120 s, 180 s and 300 s). The fluorescent probe molecule was *N*,*N*′-Bis(1-hexylheptyl)-perylene-3,4:9,10-bis-(dicarboximide) (Sigma Aldrich), which has an excitation wavelength of 523 nm and was diluted by using 1% in toluene. After impregnation, the catalyst extrudates were removed from the solution and dried in air before dividing in half and imaged with a confocal fluorescence microscopy setup. These images were measured on a Nikon Eclipse 90i instrument equipped with a 10× 0.30 NA objective. The samples were excited using a laser with a 488 nm wavelength, and the emission was collected by using an A1-DU4 4 detector system between 500–550 nm. 3-D confocal fluorescence microscopy images were composed of several 2-D images taken at different focal depths. The penetration depth of the probe molecule into the extrudate was measured manually using the microscope software. The distance between the edge of the extrudate and the location in the extrudate where the fluorescence signal was decreased to half of the intensity of the edge value was taken as penetration depth. For every data point, two catalyst extrudates were evaluated with 12 different measurements on each catalyst extrudate.

Acknowledgements

We thank Marjan Versluijs-Helder (Utrecht University, UU) for the TGA measurements as well as Oscar Kerkenaar (UU) and Ad Mens (UU) for building the operando *UV-vis microscopy setup and ExxonMobil for providing all the samples. This work was financially supported by ExxonMobil as well as by a NWO personal 'Veni' grant (722.015.003) awarded to G.T.W.*

Conflict of Interest

The authors declare no conflict of interest.

Keywords: UV-vis spectroscopy · high pressure *operando* setup · zeolites · transalkylation · *operando* microscopy

[1] A. Corma, *Chem. Rev.* **1995**, *95*, 559–614.
[2] W. Vermeiren, J.-P. Gilson, *Top. Catal.* **2009**, *52*, 1131–1161.
[3] C. Perego, P. Ingallina, *Catal. Today* **2002**, *73*, 3–22.
[4] S. Mitchell, N.-L. Michels, J. Pérez-Ramírez, *Chem. Soc. Rev.* **2013**, *42*, 6094–6112.
[5] J. S. J. Hargreaves, A. L. Munnoch, *Catal. Sci. Technol.* **2013**, *3*, 1165–1171.
[6] S. P. Verkleij, G. T. Whiting, S. P. Esclapez, M. M. Mertens, A.-J. Bons, M. Burgers, B. M. Weckhuysen, *Catal. Sci. Technol.* **2018**, *8*, 2175–2185.
[7] N.-L. Michels, S. Mitchell, J. Pérez-Ramírez, *ACS Catal.* **2014**, *4*, 2409–2417.
[8] S. Mitchell, N.-L. Michels, K. Kunze, J. Pérez-Ramírez, *Nat. Chem.* **2012**, *4*, 825–831.
[9] P. Gelin, C. Gueguen, *Appl. Catal.* **1988**, *38*, 225–233.
[10] M. W. Kasture, P. S. Niphadkar, V. V. Bokade, P. N. Joshi, *Catal. Commun.* **2007**, *8*, 1003–1008.
[11] A. Martin, H. Berndt, U. Lohse, U. Wolf, *J. Chem. Soc. Faraday Trans.* **1993**, *89*, 1277–1282.
[12] Y. Zhang, Y. Zhou, Q. Anding, Y. Wang, Y. Xu, P. Wu, *Ind. Eng. Chem. Res.* **2006**, *45*, 2213–2219.
[13] G. T. Whiting, F. Meirer, M. M. Mertens, A.-J. Bons, B. M. Weiss, P. A. Stevens, E. de Smit, B. M. Weckhuysen, *ChemCatChem* **2015**, *7*, 1312–1321.
[14] J. Ruiz-Martínez, I. L. C. Buurmans, W. V. Knowles, D. Van der Beek, J. A. Bergwerff, E. T. C. Vogt, B. M. Weckhuysen, *Appl. Catal, A* **2012**, *419–420*, 84–94.
[15] G. T. Whiting, F. Meirer, D. Valencia, M. M. Mertens, A.-J. Bons, B. M. Weiss, P. A. Stevens, E. De Smit, B. M. Weckhuysen, *Phys. Chem. Chem. Phys.* **2014**, *16*, 21531–21542.
[16] P. Castaño, J. Ruiz-Martínez, E. Epelde, A. G. Gayubo, B. M. Weckhuysen, *ChemCatChem* **2013**, *5*, 2827–2831.
[17] L. Karwacki, D. A. M. de Winter, L. R. Aramburo, M. N. Lebbink, J. A. Post, M. R. Drury, B. M. Weckhuysen, *Angew. Chem. Int. Ed.* **2011**, *50*, 1294–1298.
[18] J.-D. Grunwaldt, C. G. Schroer, *Chem. Soc. Rev.* **2010**, *39*, 4741–4753.
[19] J. Ruiz-Martínez, A. M. Beale, U. Deka, M. G. O'Brien, P. D. Quinn, J. F. W. Mosselmans, B. M. Weckhuysen, *Angew. Chem. Int. Ed.* **2013**, *52*, 5983–5987.
[20] A. J. Martin, S. Mitchell, K. Kunze, K. C. Weston, J. Pérez-Ramírez, *Mater. Horiz.* **2017**, *4*, 857–861.
[21] R. Thakur, S. Barman, R. K. Gupta, *Chem. Eng. Commun.* **2017**, *204*, 254–264.

[22] J. Hanika, Q. Smejkal, A. Krejci, J. Kolena, D. Kubička, *Pet. Coal* **2003**, *45*, 78–82.
[23] S. A. Ali, K. E. Ogunronbi, S. S. Al-khattaf, *Chem. Eng. Res. Des.* **2013**, *91*, 2601–2616.
[24] S. H. Cha, S. B. Hong, *J. Catal.*, **2018**, *357*, 1–11.
[25] A. Krejčí, S. Al-Khattaf, M. A. Ali, M. Bejblová, J. Čejka, *Appl. Catal. A* **2010**, *377*, 99–106.
[26] J. M. Serra, E. Guillon, A. Corma, *J. Catal.*, **2005**, *232*, 342–354.
[27] S. Al-Khattaf, S. A. Ali, A. M. Aitani, N. Žilková, D. Kubička, J. Čejka, *Catal. Rev. Sci. Eng.*, **2014**, *56*, 333–402.
[28] S. Al-Khattaf, M. N. Akhtar, T. Odedairo, A. Aitani, N. M. Tukur, M. Kubů, Z. Musilová-Pavlačková, J. Čejka, *Appl. Catal. A* **2011**, *394*, 176–190.
[29] J. Toda, A. Corma, G. Sastre, *J. Phys. Chem. C* **2016**, *120*, 16668–16680.
[30] S. A. Ali, A. M. Aitani, C. Ercan, Y. Wang, S. Al-Khattaf, *Chem. Eng. Res. Des.* **2011**, *89*, 2125–2135.
[31] E. Dumitriu, C. Guimon, V. Hulea, D. Lutic, I. Fechete, *Appl. Catal. A* **2002**, 237, 211–221.
[32] S. Zheng, A. Jentys, J. A. Lercher, *J. Catal.* **2006**, *241*, 304–311.
[33] J. Čejka, B. Wichterlová, *Catal. Rev. Sci. Eng.* **2002**, *44*, 375–421.
[34] S.-H. Park, H.-K. Rhee, *Catal. Today* **2000**, *63*, 267–273.
[35] H. P. Röger, K. P. Möller, C. T. O'Connor, *Microporous Mater.* **1997**, *8*, 151–157.
[36] N. M. Tukur, S. Al-Khattaf, *Energy Fuels*, **2007**, *21*, 2499–2508.
[37] M. Albahar, C. Li, V. L. Zholobenko, A. A. Garforth, *Chem. Eng. Trans.* **2017**, *57*, 907–912.
[38] S. Al-Khattaf, M. A. Ali, A. Al-Amer, *Energy Fuels* **2008**, *22*, 243–249.
[39] K. Hemelsoet, Q. Qian, T. De Meyer, K. De Wispelaere, B. De Sterck, B. M. Weckhuysen, M. Waroquier, V. Van Speybroeck, *Chem. Eur. J.* **2013**, *19*, 16595–16606.
[40] M. Guisnet, P. Magnoux, *Appl. Catal. A.* **2001**, *212*, 83–96.
[41] S. P. Verkleij, G. T. Whiting, D. Pieper, S. P. Esclapez, S. Li, M. M. Mertens, M. Janssen, A.-J. Bons, M. Burgers, B. M. Weckhuysen, *ChemCatChem* **2019**, *11*, 4788–4796.
[42] G. D. Mohr, J. P. Verduijn, *US 6,039,864 A* **2000**.
[43] H. K. Min, S. H. Cha, S. B. Hong, *ACS Catal.* **2012**, *2*, 971–981.
[44] Y. Li, H. Wang, M. Dong, J. Li, Z. Qin, J. Wang, W. Fan, *RSC Adv.* **2015**, *5*, 66301–66310.
[45] G. T. Whiting, N. Nikolopoulos, I. Nikolopoulos, A. D. Chowdhury, B. M. Weckhuysen, *Nat. Chem.* **2018**, *11*, 23–31.

Manuscript received: June 6, 2020
Revised manuscript received: July 24, 2020
Accepted manuscript online: August 7, 2020
Version of record online: September 9, 2020